Corrosion behaviour of aluminium in molten sodium

Di Zhang, Ryoichi Okuyama, Eiichi Nomura and Yuji Matsumaru
Central Laboratory, YUASA Corporation, 6-6 Josai-Cho, Takatsuki, Osaka 569 (Japan)

(Received April 29, 1993; accepted May 29, 1993)

Abstract

Sodium attack of both aluminium (99.999%, 99.8% and 99.5% purity) and Al–12wt.%Si alloy is investigated. Aluminium of 99.999% purity is immune, but aluminium of 99.8% or 99.5% purity and the Al–Si alloy are attacked by molten sodium at 350–500 °C. The corrosion product formed on the surface of the materials is identified as the AlNaSi compound. This suggests that sodium attack of aluminium and Al–12wt.%Si alloy is the result of a reaction between sodium and the silicon contained in the aluminium.

Introduction

The sodium/sulfur battery is the most well-known of the high-temperature batteries that are expected to be utilized in energy storage facilities and electric vehicles. Many studies have been carried out on this system, e.g., refs. 1–3.

Aluminium, or Al–Si alloy, is one of the structural materials of the cell design that has received significant attention. In this respect, the corrosion behaviour of aluminium in sulfur and sodium polysulfides has been studied [4–6]. By contrast, the corrosion behaviour of aluminium or Al–Si alloy in molten sodium has not been investigated in any detail. The purpose of this paper is to study the corrosion of aluminium in molten sodium, to elucidate the mechanism in the sodium attack, and to provide information about material selection that should prove useful for sodium/sulfur batteries.

Experimental

Three kinds of pure aluminium and Al–12wt.%Si alloy were used in this study. These were supplied by Kojundo Chemical Laboratory Co., Ltd. High-purity sodium was supplied by Nippon Soda Co., Ltd. The impurities contained in the aluminium-based specimens and sodium were determined by a chemical analysis method; the results are given in Table 1. Samples of pure aluminium and Al–12wt.%Si alloy, in the form of rods ($5 \times 5 \times 15$ mm), were placed in a Pyrex tube with high-purity sodium in a nitrogen atmosphere glove box, and then vacuum-sealed. Static immersion tests were conducted at 350 to 500 °C for up to about 400 h. After completion of these tests, the tubes were removed from the furnace, slowly air-cooled to room temperature, and broken apart. The sodium attached on the surface of the specimens was removed by ultrasonic washing in alcohol. The microstructure changes of the surface of the specimens were observed with a Nihon Denshi model JSM-T200 scanning electron

TABLE 1

Impurities in the specimens and sodium metal

Specimen	Impurities (ppm)							
	Fe	Si	Cu	Mn	Mg	Zn	Ti	Ca
99.999% Al	3	3	1					
99.8% Al	400	300	100	100	100	100	100	
99.5% Al	3300	700	200	200	200	200	300	
Al–12wt.%Si alloy	4				1			2
	O	C	H	Cl	Ca	K	B	
99.98% Na	12.2	5.1	0.22	5.5	3.7	40	0.5	

microscope (SEM). The corrosion product formed in the surface layer of the specimens was identified by means of X-ray diffraction analysis (XRD). A Rigaku Geigerflex-Rad II A diffractometer using Cu Kα radiation with an Ni filter at 40 kV and 20 mA was employed to obtain a strip chart recording from 2 $\theta = 25$–$70°$. The corrosion product was also analyzed with a Shimadzu model EPMA-8705 electronprobe microanalyzer (EPMA). The micro-sections were examined under an Olympus PME3 optical microscope.

Results and discussion

Electron micrographs of the surface of 99.999%Al before and after static immersion tests are given in Fig. 1. It can be seen that the surface of the aluminium is quite smooth. This indicates that aluminium of 99.999 % purity was not attacked by immersion in molten sodium at 500 °C for up to 210 h. This is because the Al–Na binary system exhibits a very low solubility of sodium in aluminium and of aluminium in sodium, and forms no compounds [7]. The coarse grains and smooth grain boundaries were seen even after the immersion tests because of the completion of the recrystallization in 99.999% Al (Fig. 1(b)).

Figure 2 presents electron micrographs of the surface of 99.8 % Al before and after the immersion tests. The surface of the aluminium becomes roughened and very small compounds with a rod shape were found to have formed either within the grain, or at the grain boundaries where pitting and intergranular corrosion occurred. It was also observed that the compounds at the grain boundaries were larger than those within the grain, and intergranular corrosion had preferentially proceeded with immersion time up to 210 h (Fig. 2(c)). Comparison of these results with those for 99.999% Al reveals that the sodium corrosion of aluminium is influenced strongly by the purity of the aluminium, and that a certain impurity contained in the aluminium plays a key role in the corrosion process. X-ray diffraction (XRD) analysis was performed to identify the structure or composition of these compounds. The XRD pattern revealed only the main peaks of aluminium, and no other peaks were obtained because the volume fraction of the compounds was too low.

The sodium corrosion behaviour of aluminium of lower purity was also investigated. Electron micrographs of the surface of 99.5% Al, before and after the immersion

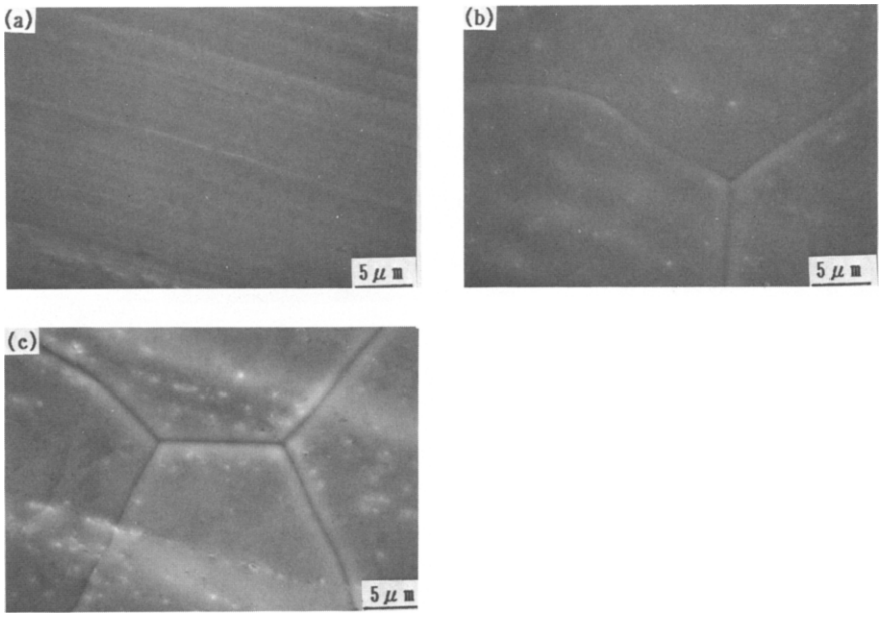

Fig. 1. Electron micrographs of the surface of 99.999% Al immersed in molten sodium at 500 °C: (a) as-received; (b) after 100 h; (c) after 210 h.

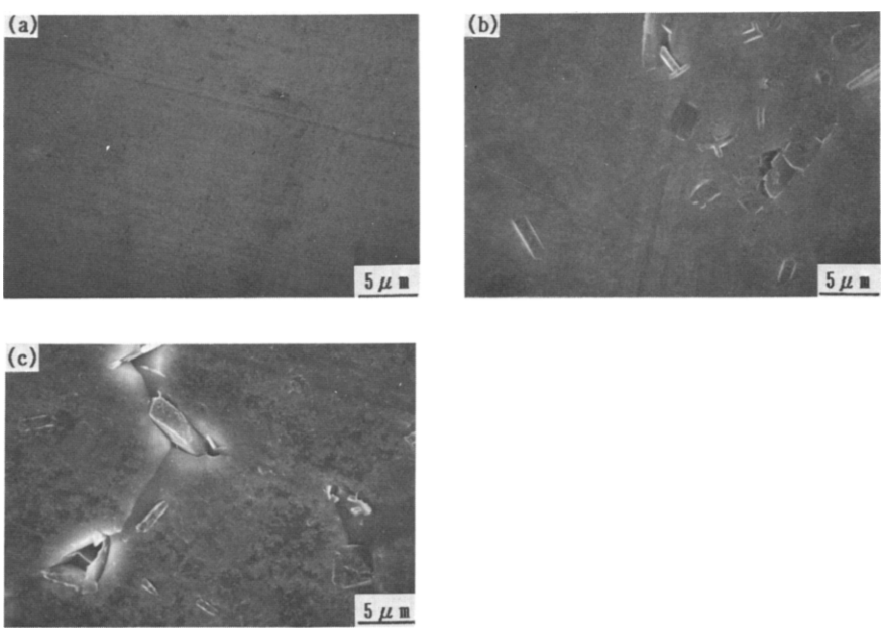

Fig. 2. Electron micrograhs of the surface of 99.8% Al immersed in molten sodium at 500 °C: (a) as-received; (b) after 50 h; (c) after 210 h.

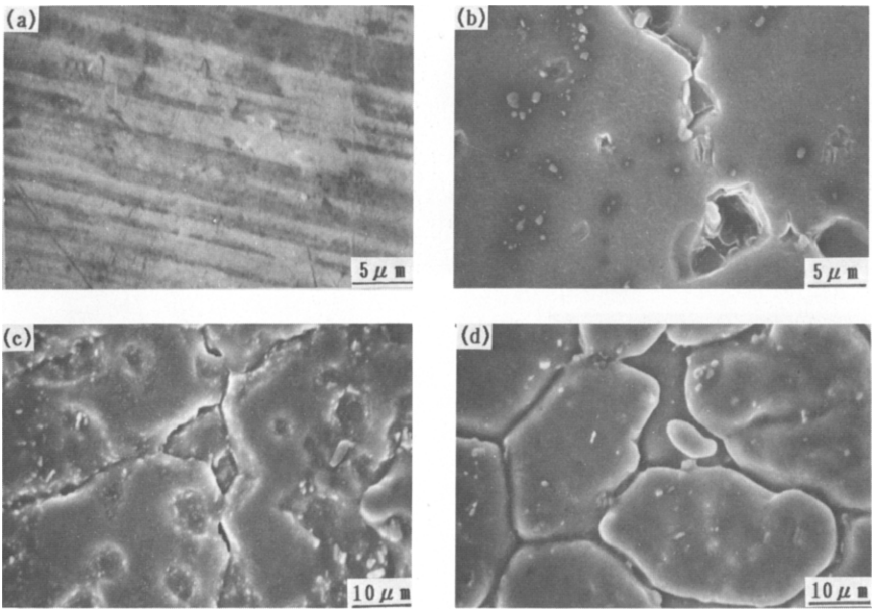

Fig. 3. Electron micrographs of the surface of 99.5% Al immersed in molten sodium at 500 °C: (a) as-received; (b) after 50 h; (c) after 100 h; (d) after 386 h.

tests at 500 °C for up to 386 h, are given in Fig. 3. The results showed that even at the initial immersion stage, 99.5% Al was attacked by molten sodium, particularly at the grain boundaries, cf., Fig. 3(b) with Fig. 3(a). Subsequently, intergranular corrosion developed, and general corrosion took place with increasing immersion time, see Fig. 3(c),(d). Compared with the behaviour of 99.8% Al, the sodium corrosion of 99.5% Al was more severe. X-ray diffraction analysis was utilized to identify the corrosion products formed on the surface of the 99.5% Al specimen. The results are shown in Fig. 4. As the immersion time increased, a few small peaks appeared in the low-angle range in addition to the main peaks for aluminium. It was difficult, however, to identify the nature of the corrosion product formed on the surface of the 99.5% Al from the small peaks obtained for a given immersion time at 500 °C. Nevertheless, when all of the small peaks were assembled together, it was found that the corrosion product was AlNaSi. This was achieved by comparing the data from the X-ray card listed in Table 2. The results (shown in Figs. 2 and 3) indicate that the silicon impurity contained in pure aluminium reacts with molten sodium to form the corrosion compound, AlNaSi. This is the nature of the corrosion of aluminium by molten sodium when commercial pure aluminium is immersed in this medium.

An electron probe microanalyzer (EPMA) was used to detect whether silicon and sodium were present in the corrosion compound formed on the surface of 99.8% Al and 99.5% Al after the sodium immersion test. The results are presented in Figs. 5 and 6. Silicon and sodium elements were detected in the corrosion compounds. For both 99.8% Al (Fig. 5) and 99.5% Al (Fig. 6) immersed in molten sodium at 500 °C for 210 and 100 h, respectively, the corrosion products usually formed at the grain boundaries. The results from the EPMA were agreement with the findings obtained from XRD analysis (Fig. 4). An iron impurity was also detected in aluminium (Fig. 6), but appeared to have no effect on the sodium corrosion behaviour of aluminium.

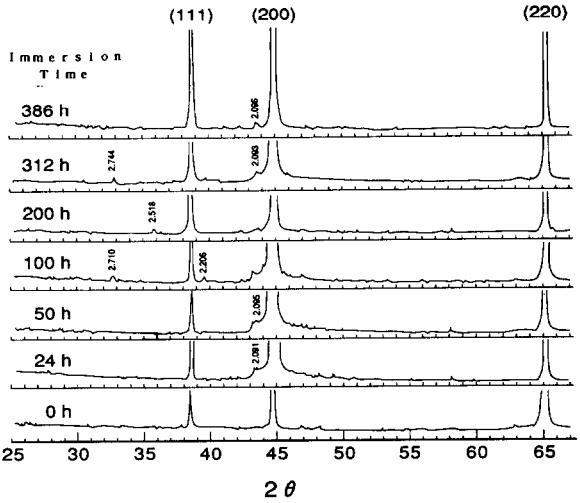

Fig. 4. X-ray diffraction patterns of 99.5% Al after immersion test in molten sodium at 500 °C for various times.

TABLE 2

X-ray data obtained from 99.5% Al immersed in molten sodium. Comparison with data in the JCPDS card for the AlNaSi compound

Temperature (°C)	d (Å)						
	2.29_x	2.72_x	2.07_8	2.75_8	7.37_6	2.11_5	1.48_3
500	2.288	2.71	2.086	2.744		2.091	

In general, the major impurities in pure aluminium are iron and silicon, and the iron has considerably more of a detrimental influence on the corrosion resistance of pure aluminium than silicon [8]. For the sodium immersion test, however, silicon exerted more of a detrimental influence on the corrosion resistance of aluminium. It is considered that the Fe–Na system is virtually immiscible in the solid and liquid states but, to date, no Fe–Na compounds have been found [9]. Although no phase diagram exists for the Si–Na systems, several compounds have been identified [10]. Thus, it should be easy to form the ternary compound AlNaSi.

In order to investigate and confirm the effect of silicon on the sodium corrosion behaviour of aluminium, an Al–12wt.%Si alloy was prepared from super-purity aluminium and high-purity silicon. The concentrations of the impurities were determined. The result of these analyses showed that, collectively, the amount of the impurities was only 7 ppm. Electron micrographs of the surface of the Al–12wt.%Si alloy before and after the immersion test at 350 °C are given in Fig. 7. Before the immersion test, the Al–Si alloy was found to have a typical eutectic microstructure, the Fig. 7(a). After the immersion in molten sodium at 350 °C, however, sodium attack occurred preferentially at the interface between the aluminium matrix and the silicon particles, Fig. 7(b). The sodium attack then proceeded vigorously and the surface of the alloy roughened in proportion to the immersion time, Figs. 7(c),(d). To identify the corrosion compounds

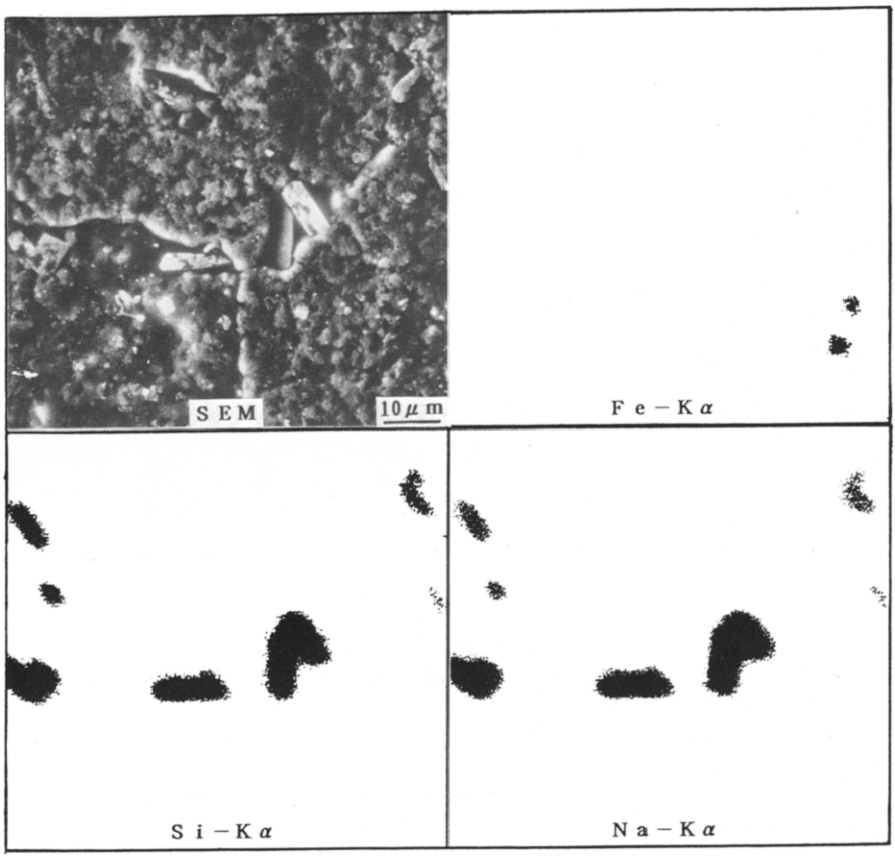

Fig. 5. Observation and analyses of 99.8% Al immersed in molten sodium at 500 °C for 210 h by SEM and EPMA.

shown in Fig. 7, XRD analysis of the Al–12wt.%Si alloy, both before and after the immersion test, was performed. The results are given in Fig. 8. It can be seen that the diffraction intensity of silicon became considerably weak and, in some cases, even disappeared, when the alloy was immersed in molten sodium at 350 °C for up to 50 h. At the same time, many new XRD peaks appeared after the immersion test, and were found to be due to the compound AlNaSi. These results were in quite good agreement with the prior results obtained from pure aluminium, as mentioned above. Examination of the Al–12wt.%Si alloy, immersed in molten sodium, confirmed that the sodium corrosion of aluminium was due to the reaction of the silicon contained in the aluminium with molten sodium to form the corrosion compound, AlNaSi.

In order to examine further the behaviour of the corrosion compound, AlNaSi, samples of the Al–12wt.%Si alloy, after immersion tests at 350 and 500 °C, were sectioned for micrographic examination by optical microscopy. The optical micrographs are given in Fig. 9. It can be seen that the corrosion compound, AlNaSi, formed as long, coarse columnar crystals that grew inwards from the surface of the alloy, and that these crystals reached almost to the zone of silicon particles that had remained in the eutectic structure. No silicon particles were present in the matrix between the corrosion compound, AlNaSi. The growth rate of the corrosion at 350 and 500 °C is

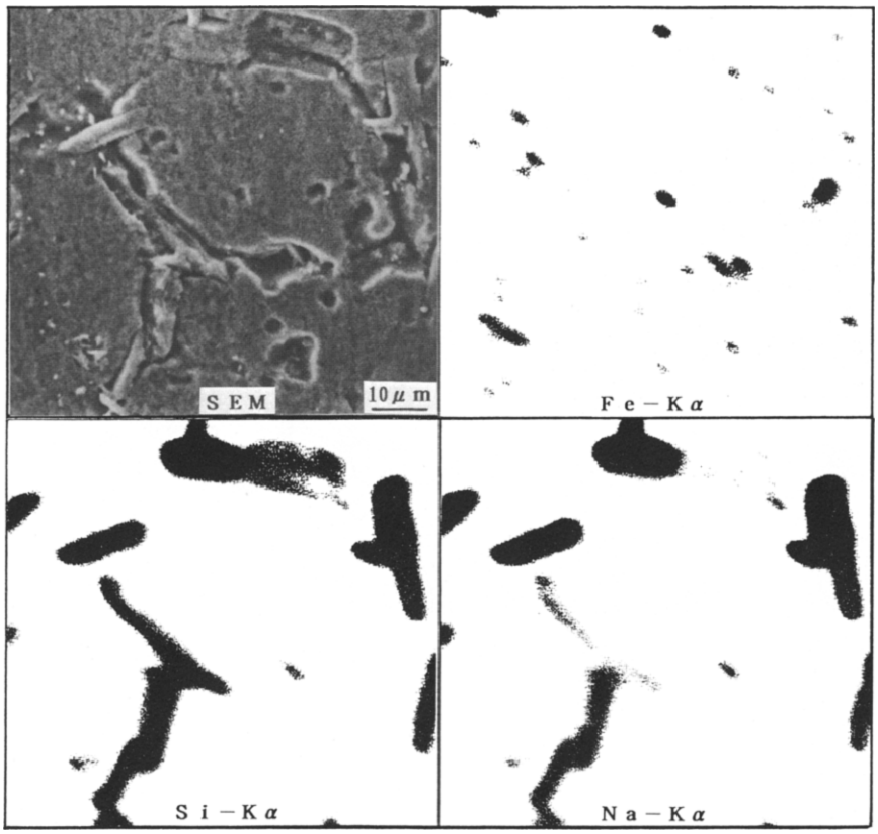

Fig. 6. Observation and analyses of 99.5% Al immersed in molten sodium at 500 °C for 100 h by SEM and EPMA.

plotted against the square root of immersion time in Fig. 10. The data in Fig. 10 show that the corrosion reaction of the alloy in molten sodium follows a parabolic rate law, i.e.:

$$X = kt^{1/2} \tag{1}$$

where X is the penetrating length of the corrosion from the surface of the Al–12wt.%Si alloy; t is the immersion time; k is a parabolic rate constant. The value of k, obtained by least-squares analyses of the data presented in Fig. 10 is 1.33×10^{-6} and 4.52×10^{-4} mm s^{-1} at 350 and 500 °C, respectively. The higher the immersion temperature, the larger the parabolic rate constant k. Using the Arrhenius equation, the diffusion activation energy of the corrosion compound, AlNaSi, was also calculated. Where Z is the rate constant (it is also proportional to the reciprocal of the immersion time t); A is a constant; R is the gas constant; T is the absolute temperature; E is the diffusion activation energy.

$$Z = A \exp(-E/RT) \tag{2}$$

A graph of log time (immersion time corresponding to the same penetration, 80 μm, of corrosion compound, AlNaSi, at 350 and 500 °C) versus 1/T is given in

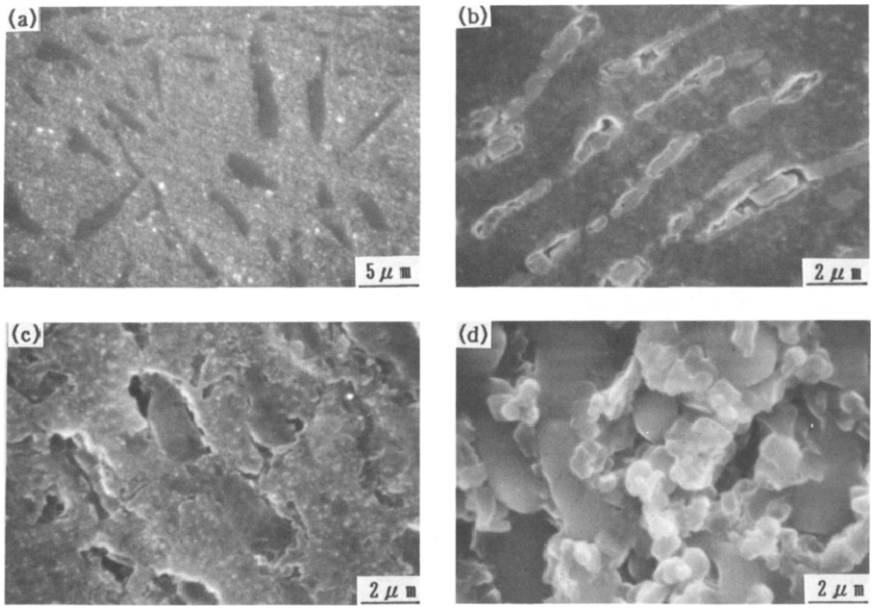

Fig. 7. SEM photographs of the surface of Al–12wt.%Si alloy immersed in molten sodium at 350 °C: (a) as-received; (b) after 24 h; (c) after 50 h; (d) after 100 h.

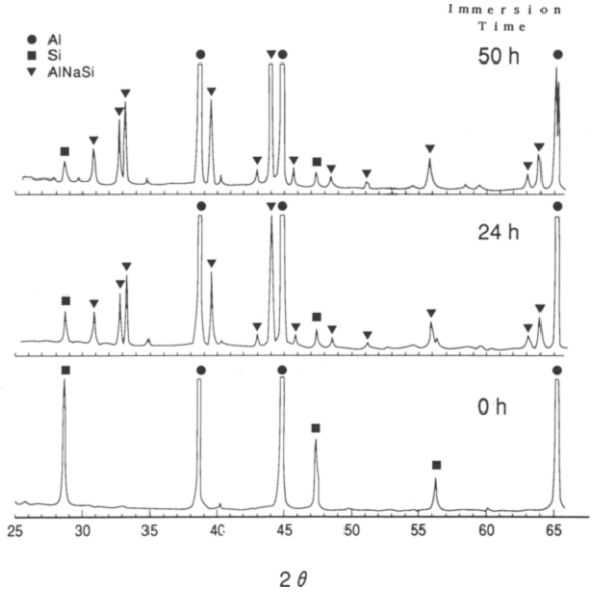

Fig. 8. X-ray diffraction patterns of Al–12wt.%Si alloy after immersion test in molten sodium at 350 °C for various times.

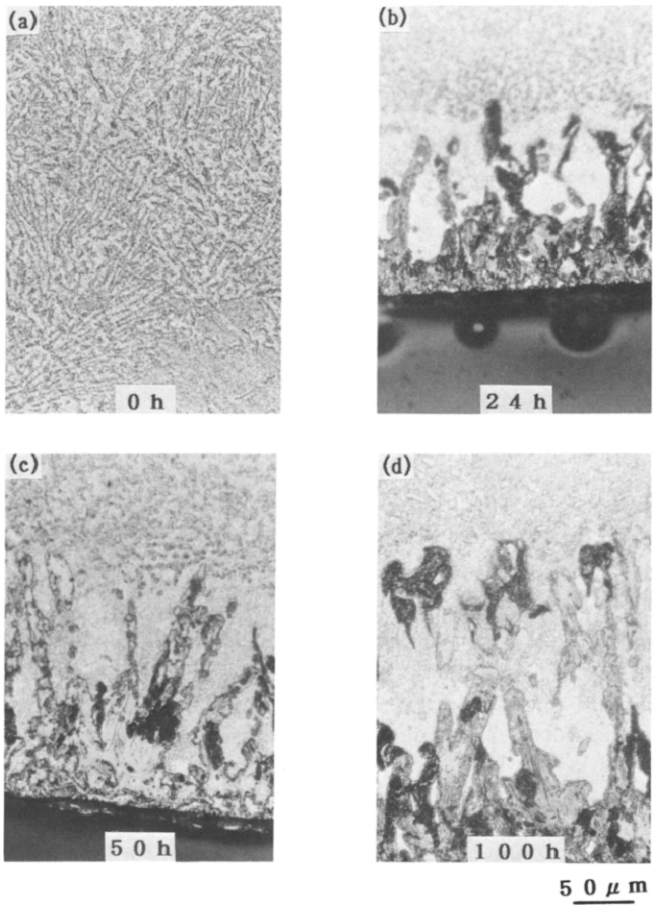

Fig. 9. Optical micrographs showing the growth of the AlNaSi phase on Al–12wt.%Si alloy immersed in molten sodium at 500 °C: (a) as-received; (b) after 24 h; (c) after 50 h; (d) after 100 h.

Fig. 11. From the slope of the line, the value of E, the diffusion activation energy, is found to be 62.4 kJ mol^{-1}. The diffusion activation energy of the corrosion compound is approximately equal to that of silicon in aluminium (i.e., $E = 76$ kJ mol^{-1}) [11], and is smaller than that of sodium in aluminium (97 kJ mol^{-1}) [12]. In fact, the diffusion rate of silicon is higher than that of sodium in aluminium at temperatures below 600 °C [13]. In other words, the diffusion rate of the corrosion compound is expected to be controlled by that of sodium in aluminium. Nevertheless, the diffusion rate of the corrosion compound, AlNaSi, obtained in Fig. 11 is higher than that of sodium in aluminium, as calculated from the published data [13]. It is assumed that silicon in aluminium promotes the diffusion of sodium. Hence, the growth rate of the corrosion compound becomes faster than the diffusion rate of sodium in pure aluminium.

Summary and conclusions

The behaviour of sodium attack of aluminium of 99.999, 99.8, 99.5% purity and Al–12wt.%Si alloy has been investigated. Aluminium of 99.999% purity is not subject

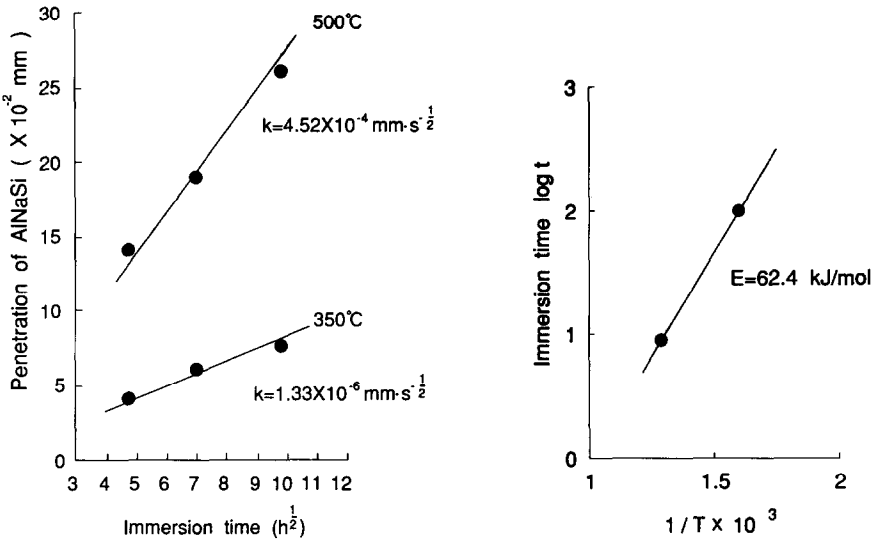

Fig. 10. Plots of the extent of corrosion vs. the square root of immersion time for Al–12wt.%Si alloy immersed in molten sodium at 350 and 500 °C.

Fig. 11. Arrhenius plots for immersion time of the AlNaSi phase, 80 μm in length.

to attack. By contrast, aluminium of 99.8 or 99.5% purity and the Al–Si alloy are attacked by molten sodium. The effect is particularly severe on the Al–12wt.%Si alloy and a very rough surface attack is clearly observed by SEM after a long immersion time at 500 °C. The results show that pitting and intergranular corrosion occurs during the initial immersion period and, subsequently, intergranular corrosion develops and general corrosion takes place. The sodium attack proceeds with increasing immersion time for 99.8% Al and 99.5% Al.

The corrosion product formed on the surface of 99.8% Al, 99.5% Al and Al–12wt.%Si alloy has been examined by XRD and EPMA. The analysis shows that the corrosion product is AlNaSi. This suggests that the sodium attack of aluminium and the alloy is due to the corrosion of silicon contained in the aluminium to produce AlNaSi. The sodium attack of aluminium is influenced strongly by the silicon content in the aluminium, and increased in severity with increasing silicon content. The formation behaviour of the corrosion compound has also been examined. For the alloy, it is found that the growth rate of AlNaSi on the alloy follows a parabolic rate law, and that the diffusion activation energy of the corrosion compound is 62.4 kJ mol^{-1}.

References

1 E. Nomura, K. Matsui, A. Kunimoto, K. Takashima and Y. Matsumara, *27th Intersociety Energy Conversion Engineering Conf. Proc., San Diego, CA, USA, Aug. 3–7, 1992*, Vol. 3, p. 3.63.

2 A.R. Tilley, in J. Sudworth (ed.), *The Sodium Sulfur Battery*, Chapman and Hall, London, 1985, p. 257.

3 B.J. McEntire, R.H. Snow and A.V. Virkar, in A.R. Landgrebe (ed.), *Sodium–Sulfur Batteries*, The Electrochemical Society, Pennington, NJ, USA, 1987, p. 95.

4 A.P. Brown, *J. Electrochem. Soc., 134* (1987) 2506.
5 B. Hartmann, *J. Power Sources, 3* (1987) 227.
6 R. Knoedler and S. Mennicke, *Electrochim. Acta, 28* (1983) 1033.
7 T.B. Massalski, *Binary Alloy Phase Diagrams*, Vol. 1, ASM International, Materials Park, OH, USA, 1990, p. 17.
8 H.P. Godard, W.B. Jepson, M.R. Bothwell and R.L. Kane, *The Corrosion of Light Metals,* Wiley, New York, 1967, p. 12.
9 T.B. Massalski, *Binary Alloy Phase Diagrams*, Vol. 2, ASM International, Materials Park, OH, USA, 1990, p. 1730.
10 T.B. Massalski, *Binary Alloy Phase Diagrams*, Vol. 3, ASM International, Materials Park, OH, USA, 1990, p. 2731.
11 S. Fujikawa, *Metall. Trans. A, 9* (1978) 1181.
12 S. Sudar, J. Csikai and M. Buczko, *Z. Metallk., 68* (1977) 11.
13 C.E. Ransley and H. Neufeld, *J. Inst. Met., 78* (1950) 25.